Geomechanics and Engineering, *Vol. 32, No. 4 (2023) 361-373*
https://doi.org/10.12989/gae.2023.32.4.361

Compressive and tensile strength behaviors of sand reinforced with fibers and natural Para rubber

Sommart Swasdi[a], Arsit Iyaruk[b], Panu Promputtangkoon[c] and Arun Lukjan*

Department of Civil Engineering, Faculty of Engineering, Rajamangala University of Technology Srivijaya
1 Ratchdamnoennok Rd, Boyang Sub-district, Muang District, Songkhla 90000, Thailand

(*Received September 17, 2021, Revised December 27, 2022, Accepted January 12, 2023*)

Abstract. This study aimed to investigate the engineering properties and mechanical behaviors of polymer-fibers treated sand. Para rubber (PR), natural fiber (NF), and geosynthetic fiber (GF) were used to reinforce poorly graded sand. A series of unconfined compressive and splitting tensile strength tests were performed to analyze the engineering behaviors and strength enhancement mechanism. The experiment results indicated that the PR-fibers mixture could firmly enhance the strength properties of sand. The stress-strain characteristics and failure patterns have been changed due to the increase of PR and fibers content. The presence of PR and fibers strengthened the sand and enhanced the stiffness and ductility behavior of the mixture. The stiffness of reinforced sand reaches an optimum state when both NF and GF are 0.5%, while the optimum PR contents are 20% and 22.5% for the mixture with NF and GF, respectively. An addition of PR and fiber into sand contributed to increasing interlocking zone and bonding of PR-sand interfacial.

Keywords: biopolymer; fiber-reinforcement; geosynthetic fiber; natural fiber; Para rubber

1. Introduction

Sandy soil has poor cohesion and low tensile strength due to its loose structure. This disadvantage caused some problems and failures in geotechnical engineering aspects such as slope protection, highway/railway embankment, soil surface erosion, and liquefaction due to earthquake (Consoli *et al*. 2011, Chang *et al*. 2015a, Liu *et al*. 2020). As a result, sand reinforcement has been studied over the last decade, and it has been discovered that the combination of chemical additives (e.g., polymer, cement, lime, and fly ash) and fiber (e.g., natural and synthetic fibers) reinforcement is the most widely used. Regarding environmentally friendly materials in geotechnical engineering applications, using biopolymers as reinforced soil materials shows more benefits for slope protection and earth stabilization (Chang *et al*. 2020). Natural rubber is a biopolymer with the chemical formula C_5H_8 and a molecular structure of *cis*-1, 4-polyisoprene derived from the Para rubber tree (Tuntiworawitt *et al*. 2005). Since it has high *cis*-bond content and molecular weight, natural rubber has excellent resilience, elasticity, abrasion resistance, and heat dispersion (Hayashi 2009). The effect of biopolymer on the mechanical properties of sandy soil has been investigated (Kavazanjian *et al*. 2009, Burbank *et al*. 2011, Anagnostopoulos *et al*. 2013, Chang *et al*. 2015b, Chang *et al*. 2016, Qureshi *et al*. 2016, Rezaeimalek *et al*. 2018, Chang *et al*. 2019, Lee *et al*. 2019, Cabalar and Demir. 2020, Kwon *et al*. 2020, Smitha *et al*. 2021). Their findings show that forming elastic and viscous membrane structures of biopolymers through physicochemical bonds between molecules and sand particles can improve shear strength, mitigating seismic-induced liquefaction, and erosion resistance.

Furthermore, Khatami and O'Kelly (2018) investigated the use of different biopolymers to prevent granulated blast-furnace slag cement particulate grouts from bleeding. They discovered that diutan gum and xanthan gum were the most effective at preventing bleeding. A remarkable increase in the California bearing ratio (CBR) value of biopolymer treated silty clay of 340% was reported by Kolay and Dhakal (2020). Regarding the tremendous potential enhancement and eco-environmental benefit of biopolymer treated sand thus, natural rubber latex (herein referred to Para rubber, PR) was attempted for this purpose. Previous research has shown that using PR strengthening improves shear strength properties and has a significant impact on the pore size distribution of poorly graded sand. Lukjan *et al*. (2018) reported that the degree of improvement of the stress ratio and shear strength parameters (e.g., cohesion, internal friction angle, dilation angle) is a function of the PR content. For instance, the stress ratio increases by about 15%, 35%, and 50% when adding PR content by 10%, 15%, and 20%, respectively. The permeability and soil-water characteristic results indicated that PR reduces the hydraulic conductivity of sand by about 3 orders of magnitude (Lukjan *et al*. 2020). Paotong *et al*. (2020)

*Corresponding author, Assistant Professor
E-mail: arun.l@rmutsv.ac.th
[a]Assistant Professor
E-mail: sswasdi@hotmail.com
[b]Lecturer
E-mail: arsit20@hotmail.com
[c]Associate Professor
E-mail: panu_pptk@hotmail.com

ISSN: 2005-307X (Print), 2092-6219 (Online)

conducted the unconfined compression test on reclaimed asphalt pavement that had been improved with PR and Portland cement. They discovered that the mixture of 5% PR and 7% cement has a high potential for use in road construction, especially in the base and subbase courses. Buritatun *et al*. (2020) reported that replacing the PR improved the engineering properties of cement-stabilized coarse-grained soil by up to 30%, 21%, and 18% for 3%, 5%, and 7% cement contents, respectively. For the flexural strength was improved up to 78%, 40%, and 29% for 3%, 5%, and 7% cement contents, respectively.

Using fibers as reinforcing materials in the soil is still attracted increasing attention in geotechnical engineering applications. As mentioned above, natural fibers (e.g., palm, coir, sisal, bamboo, and jute) and synthetic fibers (e.g., polypropylene, polyester, polyethylene, and polyvinyl alcohol) are widely used for soil reinforcement. Jamellodin *et al*. (2010) proposed the shear strength and internal friction angle of palm oil fiber-reinforced soft clay and exhibited the optimum fiber content of 0.75%. Ahmad *et al*. (2010) studied the effect of palm fiber coating with acrylic butadiene styrene polymer of the reinforced silty sand specimen under a triaxial test. They reported that coating fibers increase the shear strength of the soil due to the increase in the diameter and surface area of the fiber. They also described the increasing cohesion of about 35% of the mixture when additional palm fiber content was 0.5%. Even though the natural fibers have some drawbacks in practical applications, such as biodegradability, this issue can be resolved by chemically treating the fibers (Wei *et al*. 2018). Kurugodu *et al*. (2018) estimated a strength improvement factor (SIF) of polypropylene fiber-reinforced soil using the genetic programming (GP) approach. The results showed that the SIF increases with increasing fiber content up to 0.75%, then decreases from 0.75 to 1%. He *et al*. (2021) investigate the tensile strength characteristics of PP fiber reinforced soil with different fiber dispersion (i.e., discrete or random distribution), aspect ratio, and content (0.35%, 0.60%, and 0.85% by weight of soil). The experiment results indicated that the tensile strength increased with increasing fiber aspect ratio. Moreover, the tensile strength of the specimen conducted by random fiber distribution was higher than that discrete distribution. Armaghani *et al*. (2020) predicted soil shear strength parameters using artificial neural network (ANN)-based models and neuro-imperialism approaches. They concluded that neuro-imperialism provides a new application model for predicting the internal friction angle and cohesion of polypropylene fiber-reinforced sandy soil. The drained triaxial compression test was used by Bahrami and Marandi (2020) to investigate the effect of imposed strain level on the strength ratio of date palm fiber-reinforced sand. They stated that it is critical to be concerned with selecting the appropriate strength in practical design because the strength or strength ratio varies with strain level.

Many scholars have recently stated that using composite reinforcement materials (e.g., fiber-reinforced cemented and fiber-polymer reinforced soil) will significantly improve the engineering properties of soils. According to published literature, the benefits of such combining reinforcement soil contribute to increasing strength development, increasing ductility behavior, erosion resistance, and reduced swelling and shrinkage. For instance, Park (2011) investigated the strength and ductility characteristics of PVA fiber-reinforced cemented sand and discovered that the unconfined compressive strength increased more than threefold as the fiber ratio increased up to 1%. That ductility also increased significantly with increasing fiber ratio. Kutanaei *et al*. (2017) stated that using polyvinyl alcohol fiber-reinforced cemented sand with nanosilica increases the compressive strength and energy absorption. Lv *et al*. (2019) investigated the performance of three different fibers reinforced cemented sand mixtures, concluding that polypropylene fiber had the best improvement effect on the mechanical behavior of the cemented sand, followed by polyester fiber and polyamide fiber. Liu *et al*. (2018) found that the polyethylene polymer solution enwraps sand particles, absorbs on the basalt fiber surface, fills voids, and creates bonds in the sand-fiber mixture. The effect of PVA fiber-reinforced cemented Toyoura silty sand on shear wave velocity was discovered by Safdar *et al*. (2021). They discovered that adding 2% cement and 1% fiber content resulted in a 24% increase in shear wave velocity.

However, while the preceding PR research primarily focused on the strength behaviors of PR-cemented soil, there have been few reports on the combined behavior of PR and fiber-reinforced sand. Therefore, the purpose of this study is to investigate the engineering properties and strength behavior of sand reinforcement using liquid PR as a chemical binder and a combination of two different types of fibers: natural and synthetic fiber. A series of laboratory tests were performed, including unconfined compressive and splitting tensile strength tests. Furthermore, the combined mechanism of the PR-treated sand and PR-fibers reinforced sand were examined using a scanning electron microscopic (SEM) image.

2. Materials and experiment program

The experiment program was performed in three stages**:** Firstly, the physical properties of materials used, namely sand, Para rubber **(**PR**)**, natural fiber **(**NF**)**, and geosynthetic fiber **(**GF**)**, were characterized**.** Secondly, composite specimens were prepared for a series of mechanical tests, including PR-treated sand **(**PRTS**)**, NF-reinforced PR treated sand **(**NFRTS**)** and, GF reinforced-PR treated sand **(**GFRTS**).** Thirdly, the scanning electron microscopy test was conducted on the observed microstructure of the mixtures**.**

2.1 Materials

The experiment program was performed in three stages: Firstly, the physical properties of materials used, namely sand, Para rubber (PR), natural fiber (NF), and geosynthetic fiber (GF), were characterized. Secondly, composite specimens were prepared for a series of mechanical tests, including PR-treated sand (PRTS), NF-reinforced PR


(a) Sand


(b) Para rubber


(c) Natural fiber, NF


(d) Geosynthetic fiber, GF

Fig. 1 Materials used in the experiment

Table 1 Physical properties of sand

G_s	ρ_{min} (g/cm^3)	ρ_{max} (g/cm^3)	e_{min}	e_{max}	%Passing				D_{50} (mm)	C_c	C_u
					1.20 mm	0.60 mm	0.30mm	0.15 mm			
2.64	1.40	1.61	0.64	0.88	100	80.7	11.8	2.0	42.0	04.1	65.1

Table 2 Physical properties of liquid Para rubber (PR)

Dry rubber content (%)	Specific gravity	pH	Ammonia content (%)	Volatile Fatty Acid Number (VFA)	Viscosity (cps.)	KOH number
60.05	0.945	10.96	70.0	0.025	59.2	0.65

Table 3 Physical and mechanical properties of fibers

Fiber type	Length (mm)	Color	Shape	Density (g/cm^3)	Tensile strength (MPa)
Natural fiber, NF	20	Brown	Strip	1.40	90 - 206
Geosynthetic fiber, GF	20	White	Monofilament	1.35	1,120*

*Grab tensile strength (N)

treated sand (NFRTS) and, GF reinforced-PR treated sand (GFRTS). Thirdly, the scanning electron microscopy test was conducted on the observed microstructure of the mixtures.

Para rubber latex (Fig. 1 (b)) is a stable colloidal dispersion of polymeric materials in an aqueous medium commercially available. High ammonia centrifuged latex was used in this study with an ammonia content of 0.70%. It has a specific gravity (at 25ºC) of 0.945, dry rubber content being 60.05%. Other physicochemical parameters are summarized in Table 2.

Fibers used in this study included natural fiber (NF) and geosynthetic fiber (GF), as shown in Figs. 1(c) and (d). The oil palm fiber, extracted from an empty fruit bunch by retting process, was selected as NF. The GF was obtained from waste polypropylene textile products. Before the GF was added, the strip textile was shredded to fine filamentous and then mixes into dry sand (Consoli *et al.* 2011, Liu *et al.* 2020). The fiber contents used in the experiments were 0.5% and 1% by weight of dry sand. The fiber length and fiber content were chosen based on published research on liquid polymer and fiber-reinforced sand. The majority of the literature suggested using fibers at a dosage of not beyond 1% by weight of sand, with fiber lengths ranging from 10 to 50 mm. (e.g., Ahmad *et al.* 2010, Jamellodin *et al.* 2010, Hejazi *et al.* 2012, Liu *et al*. 2018, Liu *et al*. 2019, Sonmezer 2019, Bahrami and Marandi 2020). Furthermore, Pradhan *et al.* 2012 reported that the strength of fiber-reinforced soil with beyond 20 mm of fiber length may cause the reduction of soil–fiber interlocking. Therefore, 20 mm fiber length was selected in this experiment. The physical properties of the NF and GF are summarized in Table 3.

2.2 Specimen preparation

To investigate the effect of different PR and fibers contents on the mechanical behaviors of sand, the preparation of samples was carried out with five PR contents of 15%, 17.5%, 20%, 22.5%, and 25%, and two fiber contents of 0.5%, and 1% by weight of dry sand. Three replications of each mixture were prepared by hand-mixing the required dosage of dry sand, PR, and fibers. First, the dry sand was mixed with fibers (NF and GF), then thoroughly mixed with the PR. Finally, the sand-fiber-PR mixture for each content was filled into a cylindrical split metal mold with a 50 mm diameter and 100 mm height. Then, the specimen was compacted in three layers with 25 consecutive lifts using a tamping rod in a mold with respect to energy controlling. In addition, the sand-PR mixtures were also prepared with the same procedure. Therefore, the molding of a total of twenty-five mixtures (i.e., 25 x 3 =75 specimens) was completed.

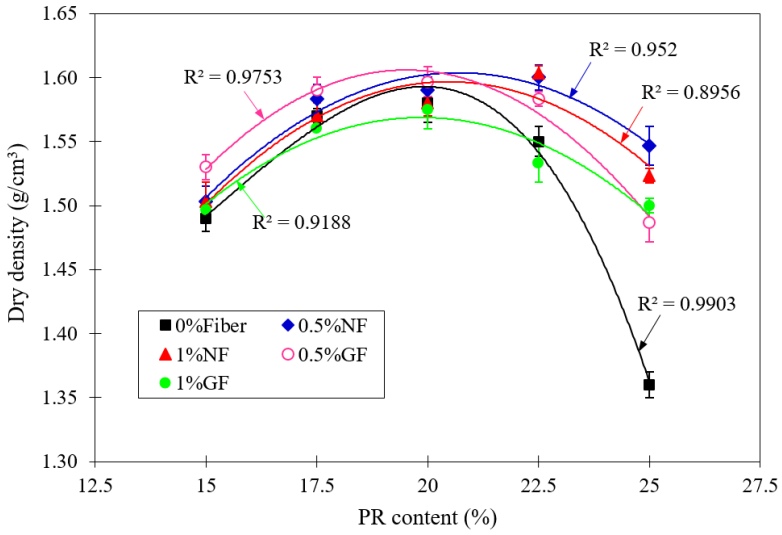

Fig. 2 The variation in the dry density with different PR and fibers contents of treated sand

After the molding process, the curing methods were considered to reduce the curing duration. In this experiment, determination of appropriate curing duration was conducted by placing and drying the molded specimens in a drying oven for 72 h. To avoid degradation of the polymer under high temperatures, the heating temperature of 100°C was selected following the suggestion of Zhang *et al*. (2015) and Rezaeimalek *et al*. (2018). After drying, there was no significant change in its mass (i.e., a mass of the samples is gradually constant after 48 h of curing time). Thus, all specimens used in this experiment were cured at 100°C for 48 h. Fig. 2 shows the variation in the dry density induced the inclusion of PR, NF, and GF contents of treated sand specimens. As shown in Fig. 2, it exhibits a similar shape to the soil compaction curve. As observed, the dry density of such specimens gradually increases with the increasing PR content. This relationship indicates that the maximum dry density reaches the optimum at the PR content of about 20%.

2.3 Testing program

2.3.1 Unconfined compression test

The 50 kN compression machine was employed to perform the unconfined compressive strength (UCS) test following the ASTM D2166 (ASTM. 2016). Before testing, the weight and dimension of the specimens were recorded. Then, a force was applied with a loading rate of 1 mm/min, and the axial deformation of each specimen was measured. Finally, the tests were terminated when the specimen reached failure or the peak stress sufficiently passed, which was at a strain less than 10% (Rezaeimalek *et al*. 2018). Additionally, the UCS tests were conducted on triplicated specimens, and an average value was reported.

2.3.2 Splitting tensile strength test

According to ASTM C 496 (ASTM. 2017), the splitting test was conducted by placing the specimen on the loading strips of the testing machine. First, the load at a constant rate of 1 mm/min was applied to the specimen, and then the maximum load was recorded. Finally, the splitting tensile strength (q_t) value was calculated using the following equation: $q_t = 2000P_{max}/\pi DL$, where the q_t is the splitting tensile strength (kPa), P_{max} is the maximum load (N), D is specimen diameter (mm), and L is the specimen thickness (mm).

3. Result and discussions

Both the UCS and splitting tests were carried out to investigate the contribution of the PR and fibers to strengthening the poorly graded sand. For the UCS test, the peak strength (q_u), residual strength (q_r), and secant modulus (E_{50}) were studied. The residual strength (q_r) is defined as the stress at failure. For the splitting test, only average values of the tensile strength (q_t) were reported. Moreover, the compressive and tension failure patterns were also evaluated in this study. All the experimental results are summarized in Table 4. The detailed analysis is given in the following section.

3.1 Unconfined compressive strength

3.1.1 Stress-strain characteristics

Duan *et al*. (2019) illustrated that the stress-strain curve behavior of fiber-reinforced cemented soil could be divided into compaction, linear, nonlinear, and failure stages. Fig. 3 shows the axial stress-strain relationships of the PRTS, NFRTS, and GFRTS specimens. As shown in Fig. 3, the stress-strain curves of all samples demonstrated that they had a similar pattern. For example, PR15GF1 in the initial stage (0 – 0.6% strain) shows the compact phase in which the strain growth rate is fast and neither dependent on the PR nor fibers content. In linear stage (0.6 – 1.9% strain), the stress-strain curve is linearity with large deformation and steep slope. Therefore, it can be inferred that strength development is mainly related to the dosage of PR and

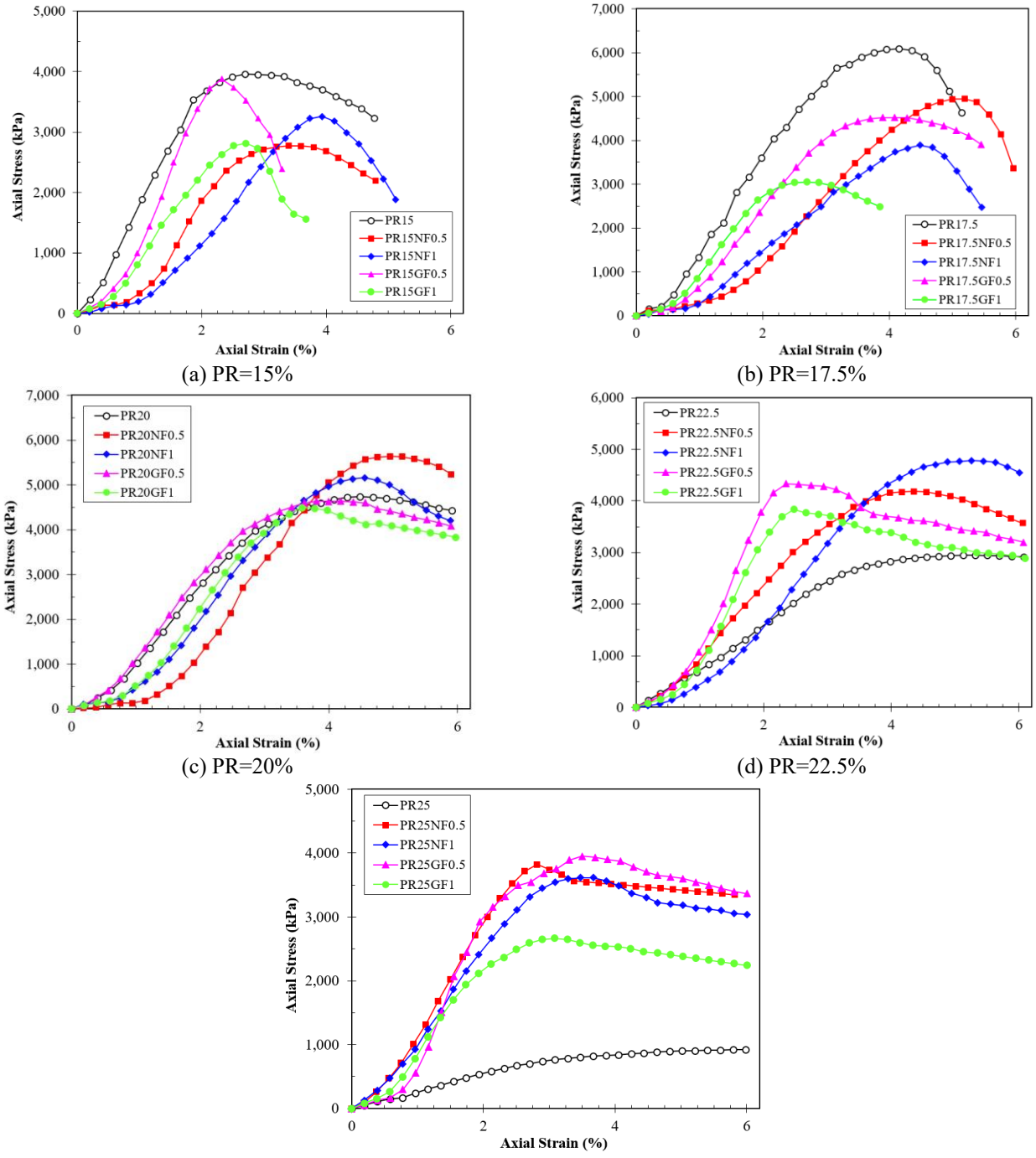

Fig. 3 The axial stress-strain curves of the PRTS, NFRTS, and GFRTS

fibers. In nonlinear stage (1.9 – 2.2% strain), the strain rate is faster than that the linear stage and the strain at peak can be observed in this stage. In the failure stage (2.2% – strain at failure), it displays a downward trend of the curve after peak stress. The post-peak feature in this stage can explain whether it exhibits brittleness or ductile behavior. The flatter curve is the toughness of the material, and the steeper slope indicates the brittleness behavior. As shown in Fig. 3, the post-peak characteristic (i.e., in failure stage) of polymer and fiber-treated sand samples shows a steep slope with an additional PR content of 15% and 17.5%. While the PR content exceeds 17.5%, the post-peak tends to be flat and exhibits a higher strain at failure, demonstrating good toughness. Thus, it can be stated that the presence of PR has a significant influence on the stress-strain characteristics.

3.1.2 Compression failure mode

The failure patterns of the cemented soil based on the study provided by Hatibu and Hettiartchi (1993) were observed during the UCS test and depicted compression failure in Figs. 4-6. As seen in Fig. 4, the brittle-slabbing failure mode was observed in the PRTS with 15% PR and

Table 4 A summary of the results under the UCS and splitting tensile tests

Mixtures	*p_c (%)	f_c (%)	q_u (kPa)	q_r (kPa)	q_t (kPa)	E_{50} (MPa)	S_r
PR15	15	-	3,955	3,234	942	179.77	0.24
PR17.5	17.5	-	6,093	4,632	1,465	179.21	0.24
PR20	20	-	4,734	4,421	1,295	131.50	0.27
PR22.5	22.5	-	2,942	2,918	650	77.42	0.22
PR25	25	-	922	950	185	30.73	0.20
PR15NF0.5	15	0.5	2,772	2,191	786	173.25	0.28
PR17.5NF0.5	17.5	0.5	4,945	3,368	1,157	154.53	0.23
PR20NF0.5	20	0.5	5,636	4,850	1,492	201.29	0.26
PR22.5NF0.5	22.5	0.5	4,185	3,568	1,594	179.46	0.38
PR25NF0.5	25	0.5	3,824	3,350	1,471	136.57	0.38
PR15NF1	15	1.0	3,256	1,882	891	125.23	0.27
PR17.5NF1	17.5	1.0	3,887	2,476	1,086	121.47	0.28
PR20NF1	20	1.0	5,160	4,205	1,364	184.29	0.26
PR22.5NF1	22.5	1.0	4,780	4,550	1,493	164.83	0.31
PR25NF1	25	1.0	3,617	3,040	1,194	139.12	0.33
PR15GF0.5	15	0.5	3,875	2,384	878	193.75	0.23
PR17.5GF0.5	17.5	0.5	4,520	3,910	972	205.45	0.21
PR20GF0.5	20	0.5	4,635	4,085	1,262	220.71	0.27
PR22.5GF0.5	22.5	0.5	4,335	3,200	1,321	264.33	0.30
PR25GF0.5	25	0.5	3,950	3,368	1,147	219.44	0.29
PR15GF1	15	1.0	2,815	1,562	785	175.94	0.28
PR17.5GF1	17.5	1.0	3,047	2,490	908	190.44	0.30
PR20GF1	20	1.0	4,487	3,830	1,340	224.35	0.30
PR22.5GF1	22.5	1.0	3,837	2,885	1,653	239.81	0.43
PR25GF1	25	1.0	2,667	2,240	1,216	166.69	0.46

*p_c : Para rubber content; f_c : Fiber content

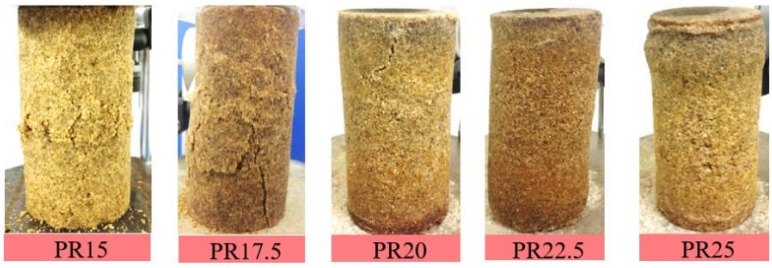

Fig. 4 Compressive failure of the PRTS

17.5% PR. In contrast, the failure mode of the PRTS seemed to be changing in ductile flow pattern when increasing PR contents exceeds 17.5%. The related stress-strain curves were mostly in good agreement with this failure behavior. Figs. 5 and 6 show the failure patterns of the NFRTS and GFRTS specimens after the UCS test, respectively. As observed, the failure pattern of the NFRTS and GFRTS with increasing fibers content were relatively similar. The samples with an additional PR content of 15% to 20% mostly show the brittle-faulting mode of failure, and the fractured area is large. However, the failure pattern of NFRTS and GFRTS containing PR contents higher than 20% gradually changes to shear-faulting mode with narrow and short fracture.

3.2 Tensile strength and failure pattern

Table 4 and Fig. 7 present the tensile strength (q_t) of treated sand specimens with different polymer and fibers contents. For the pure PR treated sand specimen, the qt increases from 942 to 1,465 kPa for the PR content increments from 15% to 17.5%. After that, it decreases from

Fig. 5 Compressive failure of the NFRTS

Fig. 6 Compressive failure pattern of the GFRTS

1,585 to 185 kPa for the PR content increases from 17.5% to 25%. As shown in Figs. 7(a) and 7(b), the q_t values for the NFRTS and GFRTS samples, as the PR content increases before 22.5%, decreases with the PR content increasing beyond 22.5%. For example, the q_t values of the specimens reinforced with 0.5% NF and the PR content with 15%, 17.5%, 20%, 22.5%, and 25% are 786 kPa, 1,157 kPa, 1,492 kPa, 1,594 kPa, and 1,471 kPa, respectively.

Figs. 8-10 displays the tension failure patterns of treated sand specimens. Fig. 8 shows the failure patterns of PRTS specimens with a variation of PR contents. As observed, the sample with PR contents of 15% and 17.5% displayed vertical failure, and the staggering crack was found in the specimen of PR20 while the samples which contained PR contents of 22.5% and 25% showed a narrow multiple and vertical cracks, respectively. Figs. 9 and 10 show cracked patterns of the NFRTS and GFRTS specimens (NF and GF content = 0.5%), respectively. The vertical, multiple, and staggered cracks were found for the NFRTS and GFRTS samples. As seen, the addition of the PR and fibers led to changes in the pattern of failures. For example, from Fig. 8, the vertical crack was found in the specimens PR15NF0.5 and PR17.5NF0.5 while the specimens PR20NF0.5 and PR22.5NF0.5 displayed multiple cracks. The staggered and multiple cracks indicated the influence of the PR and fibers in reducing the crack propagation. This aspect could be explained that when tension cracks were forming, fibers served as linking that absorbed the tensile load.

3.3 Effect of PR on strength behaviors

The mean values of q_u and q_t are shown in Table 4**.** The effect of the PR content on the strength behavior of the PRTS specimens was described through the variation of UCS **(**q_u**)** and tensile strength (q_t). As shown in Fig**.** 11, the q_u of PRTS specimens (i.e., 0% fiber) had an increasing trend within PR contents of15% to 17.5%, and the decrease in the strength was observed when the PR contents of 20%,

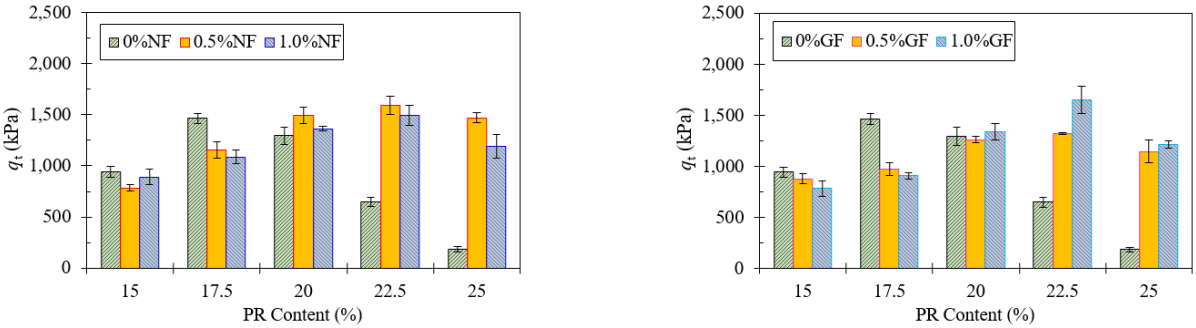

(a) PRTS and NFRTS (b) PRTS and GFRTS

Fig. 7 The splitting tensile strength of treated sand

Fig. 8 Failure pattern under spitting tension test of the PRTS

Fig. 9 Failure pattern under spitting tension test of the NFRTS

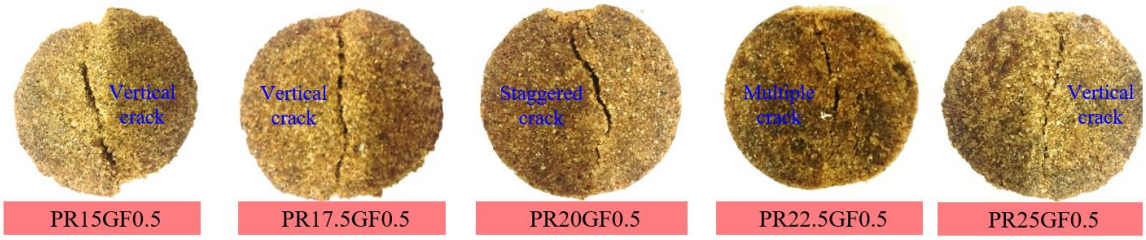

Fig. 10 Failure pattern under spitting tension test of the GFRTS

22.5%, and 25% were added. For NFRTS and GFRTS, the qu increased with the increment of PR content from 15% to 20%. Beyond 20% PR addition, a dwindling trend in the qu was observed. Thus, it can be stated that the presence of PR played a significant role in the UCS development, and that also revealed the optimum PR content (OPC) of the mixtures. As observed in Fig. 11, the OPCs based on the UCS test of the PRTS, NFRTS, and GFRTS samples are 17.5%, 20%, and 20%, respectively. The effect of PR on tensile strength can be illustrated in Fig. 7. The variation of q_t has a similar trend as the UCS, but the OPC is different. It was found that the OPCs of treated sand specimens are17.5%, 22.5%, and 22.5% for the PRTS, NFRTS, and GFRTS, respectively.

3.4 Effect of NF and GF on strength behaviors

The q_u and q_t values at the OPC were selected to describe the effect of fibers content on the strength behavior of the treated sand specimens. The q_u values at the OPC of the NFRTS specimens (Table 4 and Fig. 11(a)), with 0.5% and 1% of NF content were 5,636 kPa, and 5,160 kPa, respectively, which increased by 902 kPa (19%) and 426 kPa (9%) when compared with pure PR treated sand of 4,734 kPa. For the GFRTS specimens (Table 4 and Fig. 11(b)), the q_u of specimens with 0.5% and 1% of GF content were 4,635 kPa, and 4,487 kPa, respectively. The q_u values decreased by 99 kPa (2%) and 247 kPa (5.5%) when

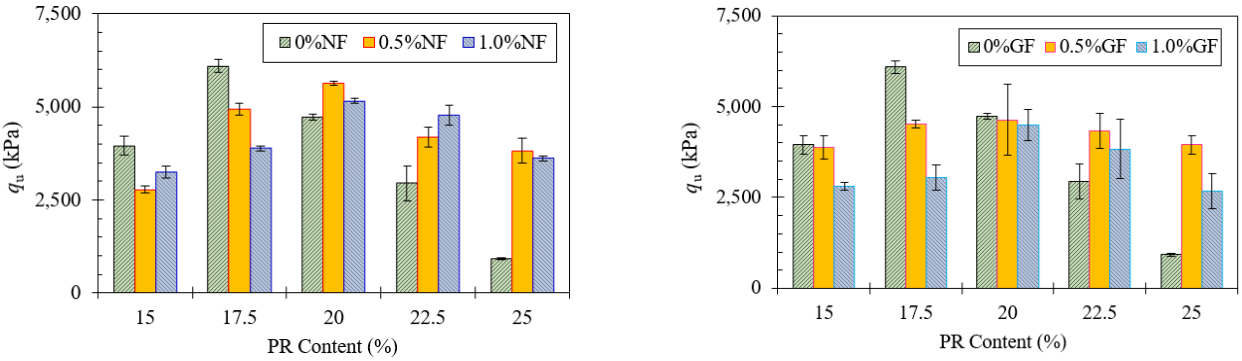

(a) PRTS and NFRTS (b) PRTS and GFRTS

Fig. 11 The unconfined compressive strength of treated sand

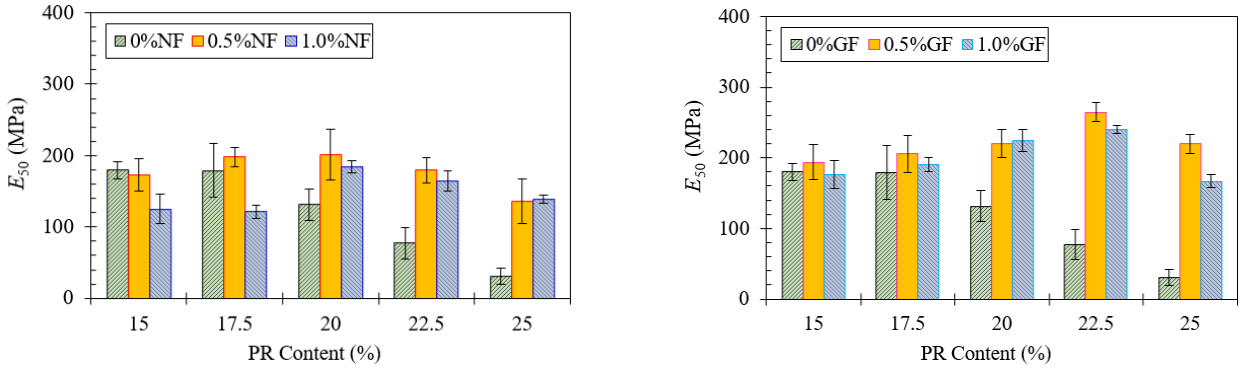

(a) PRTS and NFRTS (b) PRTS and GFRTS

Fig. 12 The E_{50} of treated sand

compared with the sample PR20. As observed in Figs. 7(a) and 7(b), the q_t of specimens PR22.5NF0.5, PR22.5NF1, PR22.5GF0.5, and PR22.5GF1 were 1,594 kPa, 1,493 kPa, 1,321 kPa, and 1,653 kPa, respectively. The q_t values increased by about 2.45, 2.30, 2.03, and 2.54 times of the specimen PR22.5, respectively. It could be described that the PR and fibers treatment led to an enhancement both in compressive and tensile strength of the treated sand specimen.

3.5 Stiffness modulus

The secant elastic modulus (E_{50}), a parameter that describes the stiffness of soil, is determined by the ratio of axial stress (at half of q_u) to its corresponding strain in the linear stage as the aforementioned. Table 4 and Fig. 12 present the E_{50} obtained from the UCS stress-strain curve of all specimens. As shown in Fig. 12, the E_{50} of 0% fiber (PRTS samples) decreased with the increasing PR contents. On the other hand, the E_{50} tends to increase in each fiber content with an increment in PR contents of 15% to 20%. After adding PR contents that exceed 20%, the reinforced specimen stiffness of each fiber content tends to reduce. This indicates that the mixture had changed its brittle behavior to a more ductile one. It can be inferred that when PR content increased to an optimum value of 20% and 22.5%, the E_{50} of the NFRTS and GFRTS specimens were enhanced, respectively. As observed in Fig. 12 and Table 4, the E_{50} of specimens PR20NF0.5 and PR20NF1 increased by about 53% and 40%, respectively, compared with the sample PR20. The E_{50} of specimens PR22.5GF0.5 and PR22.5GF1 increased by about 241% and 210%, respectively, compared with the sample PR22.5. From this result, it can be inferred that an increase of fibers in the PRTS samples can significantly increase the stiffness of the mixture as the included fibers restrain the horizontal deformation of treated sand samples. The results of the E_{50} presented above indicate that the GF provides a better stiffness than that NF.

3.6 Strength ratio analysis

The strength ratio (S_r) is defined as the ratio of tensile to compressive strength (q_t/q_u). The higher the S_r value, the better the ductile behavior (Liu *et al.* 2020). The relationship between S_r of reinforced sand is shown in Figs. 13(a) and 13(b). As shown in Fig. 13(a), the S_r of PR treated sand yielded an optimum state when PR content reached 20%. The S_r increased with NF content up to 0.5%, and afterward, it decreased slightly. For example, at 22.5% PR content, the S_r value of NFRTS increased from 0.22 to 0.38 with 0% and 0.5% NF and then reduced to 0.31 at 1% NF. It indicates that the ductility of sand is treated after the addition of NF content, not more than 0.5%. Fig. 13(b) shows the effect of the PR and GF on the S_r of the GFRTS specimens. As the PR content increased, the increasing

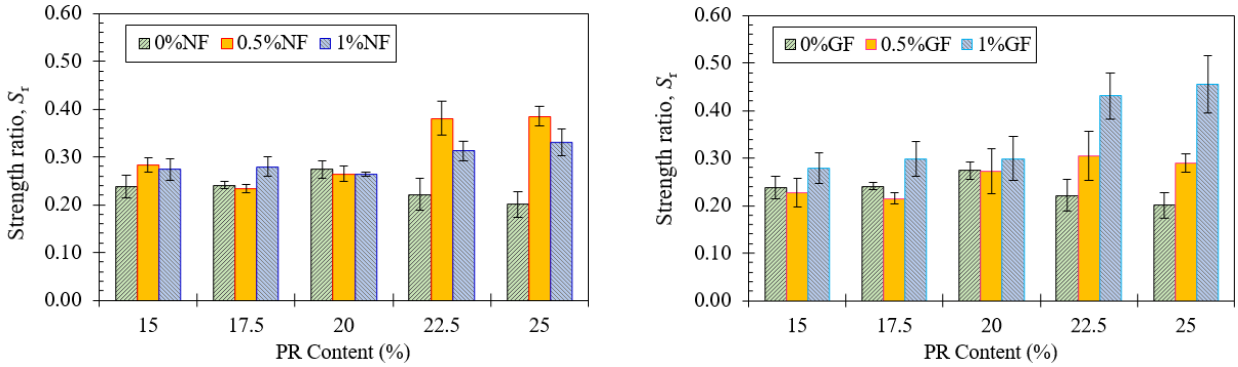

(a) PRTS and NFRTS (b) PRTS and GFRTS

Fig. 13 The strength ratio of treated sand

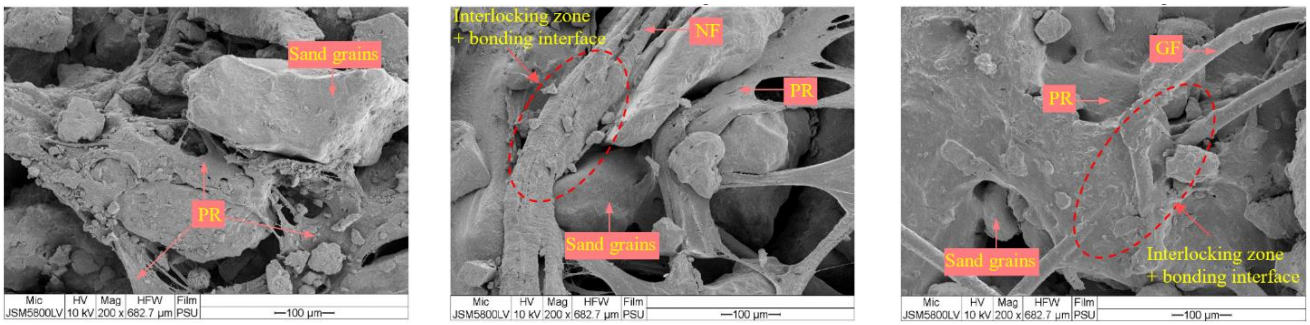

(a) PRTS (b) NFRTS (c) GFRTS

Fig. 14 SEM images of the treated sand with 200-time magnification

trend for the S_r was observed. Similarly, the S_r values also increased with increasing GF content. It is illustrated that the PR and GF play a dominant role in the strength ratio when the reinforced sand specimens are subjected to tension rather than compression, especially with the PR content that exceeds 20%.

3.7 Combined mechanism of the fibers-PR-treated sand

The microstructure of the PR treated sand and fibers-reinforced treated sand specimens were investigated by the scanning electron microscopy (SEM, JSM-5800 LV). Fig. 14 displays the SEM images of the PRTS, NFRTS, and GFRTS specimens at the magnification of 200 times. As shown in the microstructure of the PRTS in Fig. 14(a), it is clearly observed that sand grain surfaces were coated by PR. As a result, the cohesive force between sand particles effectively improved. This promoted the increase of strength and stiffness, causing the binding and confinement ability of PR film (Banjongkliang *et al*. 2015). The SEM micrographs of NFRTS and GFRTS specimens are shown in Figs. 14(b) and 14(c), respectively. As seen, the fiber surface was wrapped by PR, contributing to increasing interlocking zone and bonding of PR-sand interface. Thus, it indicates the synergy effect of PR and fibers. Previous research (e.g., Wei *et al*. 2018, Liu *et al*. 2020) also reported similar results. It is confirmed that the stiffness and strength ratio of NFRTS and GFRTS are higher than the specimen PRTS.

3.8 Possible PR treatment in geotechnical engineering practices

In Thailand, PR has been adopted in terms of soil stabilization, especially in pavement material applications (i.e., asphalt surface and granular-bound materials). Since 2017, the government of Thailand had the policy to increase PR domestic consumption due to its low price. Recently, attempts have been made to use PR to enhance the strength properties of pavement materials (e.g., Paotong *et al*. 2020, Buritatun *et al*. 2020, Kererat *et al*. 2022). The selected fiber-reinforced PR treated sand mixtures from this study were compared via those studies underlying the Thailand Department of Highway Specifications (DH-S) as shown in Fig. 15. The minimum q_u value (dashed line) for soil cement subbase (DH-S 206/2564, 2021), soil cement base (DH-S 204/2564, 2021), and cement modified crushed rock base (DH-S 203/2556, 2013) is 0.689 MPa, 1.72 MPa, and 2.41 MPa, respectively. The letters B and C refer to the contents of the bottom ash and cement, respectively. As seen in Fig.15, the q_u from the present study exhibits the highest values among others and meets all design criteria. Moreover, the additional tensile strength as the result of fibers reinforced could be reduced the tensile strain due to the traffic loads.

Thus, it can be stated that fiber-reinforced PR treated sand (i.e., NFRTS and GFRTS) displays promising potential for utilization as alternative pavement materials, especially for base course material. Despite the durability concerns in this study, Kererat *et al*. (2022) report that a soil-cement

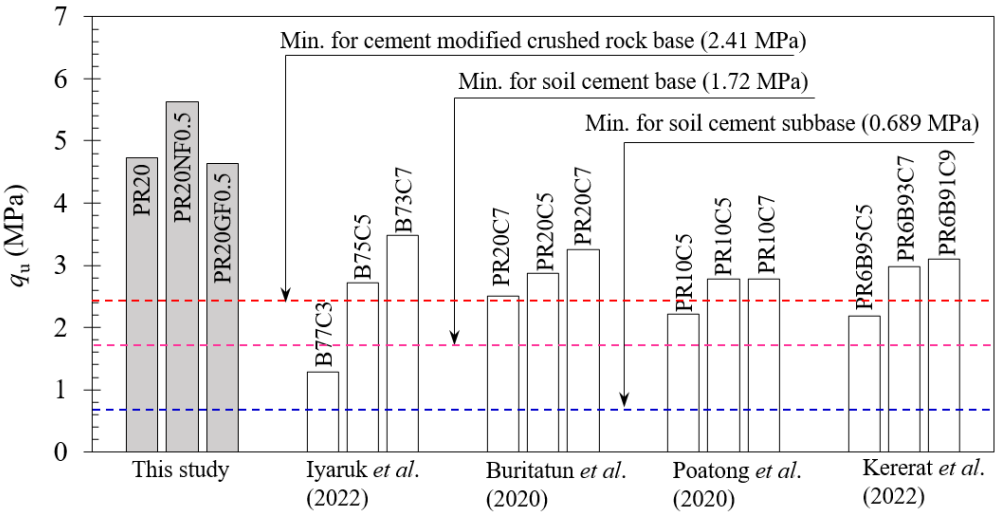

Fig. 15 The q_u of fiber-reinforced PR treated sand comparing the pavement material criteria

mixture containing PR has sufficient durability against wetting-drying cycles. However, the long-term durability of fiber-reinforced PR treated sand needs to be verified to ensure its use in practical implementation. Although the PR has a higher cost than conventional binders (e.g., cement or lime), the superior strength of such fiber-reinforced PR treated sand revealed a remarkable advantage. Therefore, more analysis in terms of economic feasibility is recommended for future research.

4. Conclusions

A series of laboratory tests, including UCS, splitting tensile, and SEM tests, were performed on fiber-reinforced PR-treated sand specimens. In addition, the effect of natural and geosynthetic fibers on the engineering properties of PR-treated sand was investigated. The findings are summarized as follows:

- The presence of PR and fibers has a significant impact on the stress-strain characteristics of the mixtures, which exhibit the typical features of treated sand specimens, including compaction, linear, nonlinear, and failure stages. The stress-strain curve generally showed strain softening at PR content of about 15% - 20% and strain hardening at PR content greater than 20%.
- The failure patterns of the reinforced sand specimens have been changed depending on their PR and fibers contents and load patterns. For compressive failure, an additional PR content of 15% to 20% mostly showed the brittle-faulting mode of failure, and the fractured area was large. The failure pattern of NFRTS and GFRTS containing PR contents higher than 20% gradually changes to shear-faulting mode with narrow and short fractures. In tensile mode, the vertical cracks, multiple cracks, and the staggered cracks were observed and it was found that when tension cracks were forming, fibers served as linking that absorbed the tensile load.
- The effects of PR-fibers reinforced sand can be explained through the result of stiffness value. The stiffness of PRTS samples decreases with the increasing PR contents. On the other hand, the stiffness increases in each fiber content with an increment in PR content of 15% to 20%. After adding PR content that exceeds 20%, the reinforced specimen stiffness of each fiber content tends to reduce, which indicates the mixture has changed its brittle behavior to a more ductile one.
- When the OPC was considered, the addition of 0.5% fiber in PR treated sand sample contributed to the increase in the stiffness. The stiffness increased by about 53% for PR20NF0.5 and 210% for PR22.5GF0.5. Moreover, the result of the E_{50} indicated the GF provides a better stiffness than the NF. The strength ratio increased with the increase of NF and GF content, indicating that the ductility of the mixtures had been improved.
- The microstructure image illustrated the combined mechanism of the fibers-PR-treated sand. As observed, the fiber surface was wrapped by PR, contributing to increasing interlocking zone and bonding of PR-sand interface.
- In summary, the additional PR content of 17.5% displayed good performance of PR-treated sand. Furthermore, the addition of NF and GF at 0.5% with a PR content of 20%, exhibited a good performance of the fiber-polymer treated sand.
- Engineering properties of PRTS, NFRTS, and GFRTS obtained in the present study indicated the feasibility for use in road application. Moreover, it may also apply to increase the bearing capacity of shallow foundations due to the shear strength parameters of sandy soil having been improved.

Acknowledgments

The authors gratefully acknowledge the Faculty of Engineering, the Rajamangala University of Technology Srivijaya (RUTS) for providing laboratory facilities in this study. Special thanks to my students, namely Mr.

Khachornkiat Phengnoo, Mr. Sittichai Eiadphanwan, and Ms. Thunyarat Khamkong for their help during laboratory testing.

References

Ahmad, F., Bateni, F. and Azmi, M. (2010), "Performance evaluation of silty sand reinforced with fibers", *Geotext. Geomembranes.*, **28**, 93–99. https://doi.org/10.1016/j.geotexmem.2009.09.017.

Anagnostopoulos, C.A., Papaliangas, T.T., Konstantinidis, D. and Patronis, C. (2013), "Shear strength of sands reinforced with polypropylene fibers", *Geotech. Geol. Eng.*, **31**, 401–423. https://doi.org/10.1007/s10706-012-9593-3.

Armaghani, D.J., Mirzaei, F., Toghroli, A. and Shariati, A. (2020), "Indirect measure of shear strength parameters of fiber-reinforced sandy soil using laboratory tests and intelligent systems", *Geomech. Eng.*, **22**(5), 397–414. https://doi.org/10.12989/gae.2020.22.5.397.

ASTM D 2166. (2016), *Standard Test Method for Unconfined Compressive Strength of Cohesive Soil*, ASTM International, West Conshohocken, PA, USA.

ASTM C 496. (2017), *Standard Test Method for Splitting Tensile Strength of Cylindrical Concrete Specimens*, ASTM International, West Conshohocken, PA, USA.

Bahrami, M. and Marandi, S.M. (2020), "Effect of strain level on strength evaluation of date palm fiber-reinforced sand", *Geomech. Eng.*, **21**(4), 327-336. http://dx.doi.org/10.12989/gae.2020.21.

Banjongkliang, E., Wattanachai, P. and Parichatprecha, R. (2015), "Evaluation of strength and microstructure of adobe stabilized with blended rubber latex and sodium silicate", *Kasetsart J. Nat. Sci.*, **49**, 288-300.

Behzadipour, H. and Sadrekarimi, A. (2021), "Biochar-assisted bio-cementation of a sand using native bacteria", *Bull Eng. Geol. Environ.*, **80**, 4967–4984. https://doi.org/10.1007/s10064-021-02235-0.

Burbank, M.B., Weaver, T.J., Green, T.L., Williams, B.C. and Crawford, R.L. (2011), "Precipitation of calcite by indigenous microorganisms to strengthen liquefiable soils", *Geomicrobiol. J.*, **28**, 301–312. https://doi.org/10.1080/01490451.2010.499929.

Buritatun, A., Takaikaew, T., Horpibulsuk., Udomchai, A., Hoy, M., Vichitcholchai, N. and Arulrajah, A. (2020), "Mechanical strength improvement of cement-stabilized soil using natural rubber latex for pavement base applications", *J. Mater. Civ. Eng.*, **32**(12), https://doi.org/10.1061/(ASCE)MT.1943-5533.0003471.

Cabalar, A.F. and Demir, S. (2020), "Fall-cone testing of different size/shape sands treated with a biopolymer", *Geomech. Eng.*, **22**(5), 441–448. https://doi.org/10.12989/gae.2020.22.5.441.

Chang, I., Prasidhi, A.K., Im, J., Shin, H.D. and Cho, G.C. (2015a), "Soil treatment using microbial biopolymers for anti-desertification purposes", *Geoderma*, **253**, 39–47. https://doi.org/10.1016/j.geoderma.2015.04.006.

Chang, I., Prasidhi, A.K., Im, J. and Cho, G.C. (2015b), "Soil strengthening using thermo-gelation biopolymers", *Constr. Build. Mater.*, **77**, 430–438. https://doi.org/10.1016/j.conbuildmat.2014.12.116.

Chang, I., Im, J. and Cho, G.C. (2016), "Geotechnical engineering behaviors of gellan gum biopolymer treated sand", *Can. Geotech. J.*, **53**(10), 1658–1670. https://doi.org/10.1139/cgj-2015-0475.

Chang, I. and Cho, G.C. (2019), "Shear strength behavior and parameters of microbial gellan gum-treated soils: From sand to clay", *Acta Geotech.*, **14**(2), 361-375. https://doi.org/10.1007/s11440-018-0641-x.

Chang, I., Lee, M., Tran, A.T.P., Lee, S., Kwon, Y.M., Im, J. and Cho, G.C. (2020), "Review on biopolymer-based soil treatment (BPST) technology in geotechnical engineering practices", *Transp. Geotech.*, **24**, 100385. https://doi.org/10.1016/j.trgeo.2020.100385.

Consoli, N.C., de Moraes, R.R. and Festugato, L. (2011), "Split tensile strength of monofilament polypropylene fiber-reinforced cemented sandy soils", *Geosynth. Int.*, **18**(2), 57–62. https://doi.org/10.1680/gein.2011.18.2.57.

DH-S 203/2556. (2013), *Standard of Cement Modified Crushed Rock Base*, Department of Highway Standard, Bangkok, Thailand.

DH-S 204/2564. (2021), *Standard of Soil Cement Base*, Department of Highway Standard, Bangkok, Thailand.

DH-S 206/2564. (2021), *Standard of Soil Cement Subbase*, Department of Highway Standard, Bangkok, Thailand.

Duan, X-L. and Zhang, J-S. (2019), "Mechanical properties, failure mode, and microstructure of soil-cement modified with fly ash and polypropylene fiber", *Adv. Mater. Sci. Eng.*, 9561794. https://doi.org/10.1155/2019/9561794.

Ham, S.M., Chang, I., Noh, D.H., Kwon, T.H. and Muhunthan, B. (2018), "Improvement of surface erosion resistance of sand by microbial biopolymer formation", *J. Geotech. Geoenviron. Eng.*, **144**(7). https://doi.org/10.1061/(ASCE)GT.1943-5606.0001900.

Hatibu, N. and Hettiaratchi, D.R.P. (1993), "The transition from ductile flow to brittle failure in unsaturated soils", *J. Agric. Eng. Res.*, **54**(4), 319–328. https://doi.org/ 10.1006/jaer.1993.1024.

Hayashi, Y. (2009), "Production of natural rubber from Para rubber tree", *Plant Biotechnol. J.*, **26**(1), 67-70. https://doi.org/10.5511/plantbiotechnology.26.67.

He, S., Wang, X., Bai, H., Xu, Z. and Ma, D. (2021), "Effect of fiber dispersion, content and aspect ratio on tensile strength of PP fiber reinforced soil", *J. Mater. Res. Tech.*, **15**, 1613-1621. https://doi.org/10.1016/j.jmrt.2021.08.128.

Hejazi, S.M., Sheikhzadeh, M., Abtahi, S.M. and Zadhoush, A. (2012), "A simple review of soil reinforcement by using natural and synthetic fibers", *Constr. Build. Mater.*, **30**, 100-116. https://doi.org/10.1016/j.conbuildmat.2011.11.045.

Iyaruk, A., Promputthangkoon, P. and Lukjan, A. (2022), "Evaluating the performance of lateritic soil stabilized with cement and biomass bottom ash for use as pavement materials", *Infrast.*, **7**(66), https://doi.org/10.3390/infrastructures7050066.

Jamellodin, Z, Talib, Z.A., Kolop, R. and Noor, N.M. (2010), "The effect of oil palm fibre on strength behaviour of soil", *Proceedings of the 3rd Southeast Asian Natural Resources and Environmental Management (SANREM) Conference*, Kota Kinabalu, Sabah, Malaysia, August.

Kavazanjian, E., Iglesias, E. and Karatas, I. (2009), "Biopolymersoil stabilization for wind erosion control", *Proceedings of the 17th International Conference on Soil Mechanics and Geotechnical Engineering*, Alexandria, Egypt, October.

Kererat, C., Kroehong, W., Thaipum, S. and Chindaprasirt, P. (2022), "Bottom ash stabilized with cement and para rubber latex for road base applications", *Case Stud. Constr. Mater.*, **17**, e01259. https://doi.org/10.1016/j.cscm.2022.e01259.

Khatami, H. and O'Kelly, B.C. (2018), "Prevention of bleeding of particulate grouts using biopolymers", *Constr. Build. Mater.*, **192**, 202-209. https://doi.org/10.1016/j.conbuildmat.2018.10.131.

Kolay, P.K. and Dhakal, B. (2020), "Geotechnical properties and

microstructure of liquid polymer amended fine-grained soils", *Geotech. Geol. Eng*., **38**, 2479-2491. https://doi.org/10.1007/s10706-019-01163-x.

Kurugodu, H., Bordoloi, S., Hong, Y., Garg, A., Garg, A., Sreedeep, S. and Gandomi, A. (2018), "Genetic programming for soil-fiber composite assessment", *Adv. Eng. Soft*., **122**, 50-61. https://doi.org/10.1016/j.advengsoft.2018.04.004.

Kutanaei, S.S. and Choobbasti. A.J. (2017), "The effects of nanosilica particle and randomly distributed fibers on the ultrasonic pulse velocity and mechanical properties of cemented sand", *J. Mater. Civ. Eng*., **29**(3). https://doi.org/10.1061/(ASCE)MT.1943-5533.0001761.

Kwon, Y.M., Ham, S.M., Kwon, T.H., Cho, G.C. and Chang, I. (2020), "Surface-erosion behaviour of biopolymer-treated soils assessed by EFA", *Géotech. Lett*., **10**, 1-7. https://doi.org/10.1680/jgele.19.00106.

Lee, S., Im, J., Cho, G.C. and Chang, I. (2019), "Laboratory triaxial test behavior of xanthan gum biopolymer-treated sands", *Geomech. Eng*., **17**(5), 445-452. https://doi.org/10.12989/gae.2019.17.5.445.

Liu, J., Bai, Y., Song, Z., Wang, Y., Chen, Z., Wang, Q., Kanungo, D.P. and Qian, W. (2012), "Effect of basalt fiber on the strength properties of polymer reinforced sand", *Fibers. Polym.*, **19**, 2372-2387. https://doi.org/10.1007/s12221-018-8507-2.

Liu, J., Wang, Y., Kanungo, D.P., Wei, J., Bai, Y., Li, D., Song, Z. and Lu, Y. (2019), "Study on the brittleness characteristics of sand reinforced with polypropylene fiber and polyurethane organic polymer", *Fibers Polym*., **20**, 620-632. https://doi.org/10.1007/s12221-019-8779-1**.**

Liu, J., Bai, Y., Song, Z., Kanungo, D.P., Wang, Y., Bu, F., Chen, Z. and Shi, X. (2020), "Stabilization of sand using different types of short fibers and organic polymer", *Constr. Build. Mater*., **253**, 119164. https://doi.org/10.1016/j.conbuildmat.2020.119164.

Lukjan, A., Iyaruk, A., Swasdi, S. and Somboon, C. (2018), "Shear strength characteristics of the natural rubber bonded sand", *Eng. J. Res. Dev.*, **29**(4), 5-18. (in Thai)

Lukjan, A., Iyaruk, A. and Somboon, C. (2020), "Soil water retention curve and permeability function of the Para rubber biopolymer treated sand", *Interdiscip, Res. Rev*., **15**(5), 1-7.

Lv, Z., Yang, Z., Zhou, H. and Zhang, S. (2019), "Mechanical behavior of cemented sand reinforced with different polymer fibers", *Adv. Mater. Sci. Eng*., **19**, 8649619. https://doi.org/10.1155/2019/8649619.

Paotong, P., Jaritngam, S. and Taneerananon, P. (2020), Use of natural rubber latex (NRL) in improving properties of reclaimed asphalt pavement (RAP)", *Eng. J*., **24**(2), 53-62. https**://**doi**.**org/10.4186/ej.2020.24.2.53.

Park, S.S. (2011), "Unconfined compressive strength and ductility of fiber-reinforced cemented sand", *Constr. Build. Mater.*, **25**(2), 1134-1138. https://doi.org/10.1016/j.conbuildmat.2010.07.017.

Pradhan, P.K., Kar, R.K. and Naik, A. (2012), "Effect of random inclusion of polypropylene fibers on strength characteristics of cohesive soil", *Geotech. Geol. Eng*., **30**, 15-25. https://doi.org/10.1007/s10706-011-9445-6.

Qureshi, M.U., Chang, I. and Al-Sadarani, K. (2016), "Strength and durability characteristics of biopolymer-treated desert sand", *Geomech. Eng*., **12**(5), 785-801. https://doi.org/10.12989/gae.2017.12.5.785.

Rezaeimalek, S., Nasouri, R., Huang, J. and Sazzad, B-S. (2018), "Curing method and mix design evaluation of a styrene-acrylic based liquid polymer for sand and clay stabilization", *J. Mater. Civ. Eng*., **30**(9), 04018200**.** https://doi.org/10.1061/(asce)mt.1943-5533.0002396.

Safdar, M., Newson, T., Schmidt, C., Sato, K., Fujikawa, T. and Shah, F. (2021), "Shear wave velocity of fiber reinforced cemented Toyoura silty sand", *Geomech. Eng*., **25**(3), 207-219. http://dx.doi.org/10.12989/gae.2021.25.3.207.

Smitha, S., Rangaswamy, K. and Keerthi, D.S. (2021), "Triaxial test behaviour of silty sands treated with agar biopolymer", *Inter. J. Geotech. Eng*., **15**(4), 484-495. https://doi:10.1080/19386362.2019.1679441.

Sonmezer, Y.B. (2019), "Investigation of the liquefaction potential of fiber-reinforced sand", *Geomech. Eng*., **18**(5), 503-513. https://doi.org/10.12989/gae.2019.18.5.503.

Tuntiworawit, N., Lavansiri, D. and Phromsorn, C. (2005), "The modification of asphalt with natural rubber latex", *J. East. Asia Soc. Transp. Studies.*, **5**, 679-694.

Wei, J., Kong, F., Liu, J., Chen, Z., Kanungo, D.P., Lan, X., Jiang, C. and Shi, X. (2018), "Effect of sisal fiber and polyurethane admixture on the strength and mechanical behavior of sand", *Polym*., ***10***, 1121. https://doi.org/10.3390/polym10101121.

Zhang, Z., Zhu, W., Zhang, J. and Tian, T. (2015), "Highly toughened poly (acrylonitrile styrene acrylic)/chlorinated polyethylene blends: mechanical, rheological and thermal properties", *Polym. Test*., **44**, 23-29. https://doi.org/10.1016/j.polymertesting.2015.03.017.

IC